Astrophysical Journal Letters, accepted, 23 November 1999

Detection of Planetary Transits Across a Sun-like Star

David Charbonneau [1,2], Timothy M. Brown [2], David W. Latham [1], and Michel Mayor [3]

ABSTRACT

We report high precision, high cadence photometric measurements of the star HD 209458, which is known from radial velocity measurements to have a planetary mass companion in a close orbit. We detect two separate transit events at times that are consistent with the radial velocity measurements. In both cases, the detailed shape of the transit curve due to both the limb darkening of the star and the finite size of the planet is clearly evident. Assuming stellar parameters of 1.1 $R_\odot$ and 1.1 $M_\odot$, we find that the data are best interpreted as a gas giant with a radius of 1.27 ± 0.02 $R_{\rm Jup}$ in an orbit with an inclination of $87.1 \pm 0.2°$. We present values for the planetary surface gravity, escape velocity, and average density, and discuss the numerous observations that are warranted now that a planet is known to transit the disk of its parent star.

Subject headings: planetary systems – stars:individual(HD 209458) – binaries: eclipsing – techniques: photometric – techniques: radial velocities

1. INTRODUCTION

Radial velocity surveys of nearby F, G, K and M dwarf stars have revealed a class of close-in extrasolar massive planets that orbit their stars with an orbital separation of $a \lesssim 0.1$ AU. There are currently eleven such candidates known (Mayor & Queloz 1995; Butler et al. 1997; Butler et al. 1998; Fischer et al. 1999; Mayor et al. 1999; Queloz et al. 1999; Udry et al. 1999; Mazeh et al. 2000). Prior to the transit results on this star, the radial velocity method has been the only method by which we have learned anything about these planets. The radial velocity technique measures the period, semi-amplitude, and eccentricity of the orbit, and by inference the semi-major axis and minimum mass, dependent upon the assumed value for the stellar mass. The search to measure the transit photometrically is motivated by fact that, for a star for which both the radial velocity and transits are observed, one can estimate both the mass (with negligible error due to $\sin i$) and radius of the planet. These can then be combined to calculate such critically interesting quantities as the surface gravity and average density of the planet, and thus provide the first constraints on structural models for these low-mass companions. Assuming a random alignment of the orbital inclination to the line-of-sight for a system with $a = 0.05$ A.U., the chance of a transiting configuration is roughly 10%, depending upon the value of the stellar radius.

[1]Harvard-Smithsonian Center for Astrophysics, 60 Garden Street, Cambridge, MA 02138; dcharbonneau@cfa.harvard.edu, dlatham@cfa.harvard.edu

[2]High Altitude Observatory, National Center for Atmospheric Research, P. O. Box 3000, Boulder, CO 80307-3000; timbrown@hao.ucar.edu. The National Center for Atmospheric Research is sponsored by the National Science Foundation.

[3]Observatoire de Genève, CH-1290 Sauverny, Switzerland; Michel.Mayor@obs.unige.ch

In this letter, we present observations of the photometric dimming of HD 209458, which we attribute to the passage of the planet across the stellar disk. Observations of this star covering less than one full transit have also recently been reported by Henry et al. (1999). Motivation for observing HD 209458 came from D. W. Latham and M. Mayor (personal communication) in August 1999. The star had been observed both on Keck I with HIRES (Vogt et al. 1994) and with ELODIE on the 1.93-m telescope at Observatoire de Haute Provence (Baranne et al. 1996) as one of the targets in two independent searches for extrasolar planets. When the two teams discovered that they had both detected low-amplitude velocity variations, they agreed to pool their efforts. Additional observations were then obtained with CORALIE on the new 1.20-m Swiss telescope at La Silla (Queloz et al. in preparation). The preliminary orbital solution from the combined data was then used to predict times of transit for the photometric observations. A proper interpretation of the transit results requires accurate estimates of the mass, radius, and limb darkening of HD209458, and of the observed radial velocity amplitude of the primary. These issues are addressed in a companion paper (Mazeh et al. 2000, henceforth M00). In what follows, we have used parameters of HD209458 and of its radial velocity orbit from this source except as noted.

2. OBSERVATIONS AND DATA REDUCTION

We undertook a program to observe HD 209458 both to establish that the star was photometrically stable for the majority of its orbit (and thus support the hypothesis that the observed radial velocity variations were due to an orbiting companion and not due to some form of stellar variability), and to search for planetary transits. We obtained photometric observations using the STARE Project Schmidt camera (focal length = 286 mm, f/2.9), which images a field 6° square onto a 2034 × 2034 pixel CCD with 15 μ pixels. This camera was designed to search for planetary transits in large samples of stars; it is described more fully in Brown & Kolinski (1999).

We observed HD 209458 for ten nights (UT dates 29, 30 Aug, & 1, 6-9, 11, 13, 16 Sep 1999). In order to avoid saturation from the high flux from the star ($V = 7.65$), we defocused the telescope. The resulting distorted point spread function caused no problems, as we later analyzed the images by means of aperture photometry. All measurements were made through a red (approximately Johnson R) filter, with the exception of some images on 29 Aug that were taken in both V and B to estimate stellar colors.

The times at which a potential transit could occur were calculated from the preliminary orbital period and ephemeris from M00. The important elements were the orbital period P and the time of maximum radial velocity of the star $T_{\rm max}$. For this Letter, we have analyzed four nights of data; two of these (29 Aug & 13 Sep) occur off transit and establish the non-variability of the star, while two (9 and 16 Sep) encompass the time of transit. We produced calibrated images by subtracting a master bias and dividing by a master flat. Sixteen images from 16 Sep were averaged to produce a master image. We used DAOPHOT II (Stetson 1994) to produce a master star list from this image, retaining the 823 brightest stars. For each time series image, we then estimated a coordinate transformation, which allowed for a linear shift δx and δy. We then applied this coordinate transformation to the master star list and carried out aperture photometry for all the images. For each star, a standard magnitude was defined from the result of the aperture photometry on the master image. We corrected for atmospheric extinction using a color-dependent extinction estimate derived from the magnitudes of the 20 brightest stars in the field (excluding HD 209458 and two obviously variable stars). For two of the nights of data (29 Aug & 13 Sep), the residuals for HD 209458 are consistent with no variation. However, on the other nights (9 Sep & 16 Sep), we can see a conspicuous dimming of the star for a time of several hours. These residuals are shown in Figure 1. The root mean square (RMS) variation in the resulting time series at the beginning of the night of 9 Sep is 4 mmag; the dominant source of noise for these bright stars is atmospheric scintillation.

3. ANALYSIS OF LIGHT CURVE

3.1. Orbital Parameters

As presented in M00, the derived orbital parameters from the combined radial velocity observations are $P = 3.52447 \pm 0.00029$ d and $T_{\max} = 2451370.048 \pm 0.014$ HJD.

Since we observed two transits, it is possible to estimate independently both a period and the time at the center of the transit, T_c, for the orbit. To derive the period, we phased the data to an assumed P value, in a range surrounding 3.5 d, and interpolated the data from the first transit onto the grid of observation times for the later transit. The weighted sum of the square of the difference was calculated as a function of assumed period, resulting in a clear minimum and a well defined error. We find the orbital period to be $P = 3.5250 \pm 0.003$ d, consistent with but less precise than the value determined from the radial velocity observations. As discussed in M00, the best fit value of the mass for this star is $M_s = 1.1 M_{\odot}$; assuming this value, we determine the semimajor axis to be $a = 0.0467$ A.U..

We used the data from the earlier transit, which was the more precisely observed, to determine T_c. For each assumed value of T_c, we folded the light curve about T_c and calculated the weighted sum of the square of the difference between the two halves of the folded curve. We find that $T_c = 2451430.8227 \pm 0.003$ HJD. This value is consistent with but is much more tightly constrained than the value determined from the radial velocity observations.

Projecting the errors in P from the radial velocity observations and T_c from the photometry observations, the time of transit can be calculated with a precision of better than half an hour for the next six months.

3.2. Interpretation of the Transit Curve

For the purpose of interpreting the light curve, we binned the residuals from both transits into 5 minute time bins according to the orbit derived above. The time series RMS of these binned data is 1.5 mmag throughout the timespan covered by the observations, with an increase to larger scatter roughly 1 hour after the point of last contact due to the increasing airmass. These binned data are plotted in Figure 2.

Five parameters participate in determining the precise shape of the transit curve. These are the planetary radius R_p, the stellar radius R_s, the stellar mass M_s, the orbital inclination angle i, and the limb darkening parameter c_λ, where the normalized stellar surface brightness profile is written as $B_\lambda(\mu) = 1 - c_\lambda(1 - \mu)$, and μ is the cosine of the angle between the normal to the stellar surface and the line-of-sight. Though they are physically distinct, not all of these parameters have independent influences on the light curve. To estimate these parameters, we adopt the following approach. Absent photometric observations, there are no observational data to restrict R_p and i, whereas there is a wealth of information on R_s, M_s, and c_λ from the theory of stars and the observed values of the star's brightness, color, metallicity, temperature, and age. A detailed presentation of the best fit values for R_s, M_s, and c_λ is given in M00. From a preliminary investigation, we adopt $R_s = 1.1\ R_{\odot}$ and $M_s = 1.1\ M_{\odot}$, consistent with the G0 V spectral type of the star. The photometry we present here was taken in the R band, for which we take $c_R = 0.5$, the solar value (Allen 1973).

We modeled the data as follows. For each assumed value of $\{R_p, i\}$, we calculated the relative flux change at the phase of each observation by integrating the flux occulted by a planet of given radius at the correct projected location on a limb-darkened disk, computing the integral over the unobstructed disk, and forming the ratio. A detailed description of the form of this integral can be found in Sackett (1999). We then calculated the χ^2 of the model applied to the 5 m phase binned time series. A contour plot of this χ^2 surface appears in Figure 3.

Adopting $\{R_s, M_s\} = \{1.1,\ 1.1\}$ (solar units), the best fit values for the parameters are $R_p = 1.27 \pm 0.02\ R_{\rm Jup}$ and $i = 87.1 \pm 0.2°$. The uncertainties quoted correspond to the 1-σ contour in the χ^2 surface. These are not, however, correct estimates of the true uncertainties. The uncertainty in the physical parameters of the star, namely R_s, M_s, and c_R, cause uncertainties in R_p and in i that exceed the stated formal errors. The systematic effect due to an uncertainty in either M_s or c_R is small. In particular, holding the stellar radius and mass constant, and changing the value of c_R by ± 0.1 changes the best-fit value of i by $\pm 0.15°$ and R_p by $\pm 0.01\ R_{\rm Jup}$. In contrast to this, the effect due to the uncertainty in R_s is significant. In Figure 3, we show the confidence ellipses for several choices of stellar mass and radius. This demonstrates the fashion in which a larger star would require a larger planet at a lower inclination to adequately fit the data. We note, however, that no plausible values of the stellar radius or mass give R_p as large as 1.6 $R_{\rm Jup}$, the value presented by Henry et al. (1999).

4. DISCUSSION

Since we have measured the orbital inclination, we can estimate the true mass of the planet. Using our measured value $i = 87.1°$, we derive $M_p = 0.63\ M_{\rm Jup}$.

The derived value of $R_p = 1.27\ R_{\rm Jup}$ is in excellent agreement with the early predictions of Guillot et al. (1996), who calculated the radius for a strongly irradiated radiative/convective extrasolar planet for a variety of masses.

Since this is the first extrasolar planet of a known radius and mass, several physically important quantities can be calculated for the first time. We estimate an average density of $\rho \approx 0.38\ {\rm g\,cm^{-3}}$, which is significantly less than the density of Saturn, the least dense of the solar system gas giants. The surface gravity is $g \approx 970\ {\rm cm\,s^{-2}}$. Assuming an effective temperature for the star of $T_s = 6000K$, and a planetary albedo of A, the effective temperature of the planet is $T_p \approx 1400\ (1 - A)^{\frac{1}{4}}\ K$. This implies a thermal velocity for hydrogen of $v_t \lesssim 6.0\ {\rm km\,s^{-1}}$. This is roughly a factor of 7 less than the calculated escape velocity of $v_e \approx 42\ {\rm km\,s^{-1}}$, confirming that these planets should not be losing significant amounts of mass due to the effects of stellar insolation.

The existence of a transiting planet suggests many fruitful observations that bear on both planetary and stellar physics.

It will be highly desirable to obtain high cadence photometry of similar precision in as many band passes as possible. Observing the color dependence of the transit shape will measure the limb darkening, and break the degeneracy shared between this effect and the other parameters. In particular, we predict a deeper transit in V and B, due to greater limb darkening at these shorter wavelengths.

If there are other planets in the HD 209458 system, and if their orbits are approximately coplanar with the one we observe, then the likelihood that they too will generate transits is substantially enhanced relative to that for a randomly oriented system. The radial velocity data of M00 do not suggest other massive objects in this system. However, less massive objects (similar to Uranus, for instance) could easily escape detection via radial velocities, and yet be observable photometrically. Gilliland and Brown (1992) showed that observations with a 2-m telescope could attain precision of 400 μmag per minute of integration. A central transit by a Uranus-sized planet at 0.2 AU would yield a dimming some 6 hours in duration, with a depth of about 1 mmag; this would be easily visible with the abovementioned precision. With the accuracy that should be attainable from outside the Earth's atmosphere (eg., Borucki et al. 1997), planets the size of Earth would be detectable. Note, however, that in the case of exactly coplanar orbits, the orbital inclination of 87.1° implies that planets further than 0.1 AU from the star will show no transits. From this point of view, a small dispersion in orbital inclination would enhance, not decrease, the chances of observing other planets.

Other objects in the HD209458 system need not be separate planets; they could be moons of the known planet, or even dust rings surrounding it. Dynamical considerations restrict the allowable distance of such bound objects from the planet, simplifying the detection problem. Precise photometric searches for such objects could in principle yield detections for moons only slightly larger than the Earth.

Reflected light observations such as those for the τ Boo system by Charbonneau et al. (1999) and Cameron et al. (1999) will be difficult, because of the relative faintness of this star. If successful, however, they would yield the planet's albedo directly, since its radius is accurately known. In particular, the ratio of the flux from the planet at opposition to that of the star is $\sim 1.7 \times 10^{-4}\ p_\lambda$, where p_λ is the wavelength dependent geometric albedo. Similarly, observations at wavelengths longer than a few microns may detect the secondary eclipse as the planet passes behind the star. In the long wavelength limit, the depth ratio of the primary to the secondary eclipse should be the ratio of the effective temperatures, roughly 4, leading to signals of perhaps 3 mmag. Knowing this depth would allow the planet's actual dayside temperature to be estimated, hence constraining the mean atmospheric absorptivity.

Differences between spectra of the star in and out of transit would reveal changes in the line depths at roughly the 1% level due to the variations in the line profile integrated over the visible surface of the partially occulted star. At a level of roughly 0.01%, it may be possible to observe absorption features added by the planetary atmosphere while it is in transit. The atmospheric scale height will be greatly enhanced due to the high temperature of the planet, and this effect may bring the amplitude of the absorption features into the observable regime. Charbonneau et al. (1999) have demonstrated that time varying changes in the spectrum of the system can be monitored at the level of better than 5×10^{-5} for the bright star τ Boo. If this technique can be extended to this star, it would be possible to search for these absorption features.

5. CONCLUSION

The discovery of transits in the light curve of HD209458 confirms beyond doubt that its radial velocity variations arise from an orbiting planet. Moreover, having a reliable estimate of the planetary radius and mass, we can now say with assurance that the planet is indeed a gas giant. We are encouraged by the closeness of the fit between our observed radius and that computed on theoretical grounds by Guillot et al. (1996). One may nonetheless expect that observations of this and similar systems will rapidly become more sophisticated and penetrating, and that the results will be puzzling more often than not. We are confident that solving these puzzles will lead to a new and far more comprehensive understanding of the processes that control the formation and evolution of planets, and to an exciting time for those with an interest in the field.

The identification of HD 209458 as a prime target for transit observations was made possible by the many contributions of the members of the G Dwarf Planet Search, ELODIE, and CORALIE teams: J. L. Beuzit, M. Burnet, G. A. Drukier, T. Mazeh, D. Naef, F. Pepe, Ch. Perrier, D. Queloz, N. Santos, J. P. Sivan, G. Torres, S. Udry, and S Zucker. We are especially grateful to T. Mazeh and the members of his team in Tel Aviv for their critical role in the analysis of the Keck observations. We are grateful to R. Noyes for many helpful conversations, and we thank the referee E. Dunham for helpful comments, which improved the paper. Furthermore, we thank G. Card, C. Chambellan, D. Kolinski, A. Lecinski, R. Lull, T. Russ, and K. Streander for their assistance in the fabrication, maintenance, and operation of the STARE photometric camera. We also thank P. Stetson for the use of his DAOPHOT II software. D. Charbonneau is supported in part by a Newkirk Fellowship of the High Altitude Observatory. This work was supported in part by NASA grant W-19560.

REFERENCES

Allen, C. W. 1973, Astrophysical Quantities, 3rd ed, Athlone Press, London

Baranne, A., Queloz, D., Mayor, M., Adrianzyk, G., Knispel, G., Kohler, D., Lacroix, D., Meunier, J.-P., Rimbaud, G., & Vin, A. 1996, A&AS, 119, 373

Borucki, W., Koch, D., & Webster, L. 1997, Kepler Mission: A Search for Habitable Planets, proposal to NASA

Brown, T. M. & Kolinski, D. 1999, http://www.hao.ucar.edu/public/research/stare/stare.html

Butler, R. P., Marcy, G. W., Williams, E., Hauser, H., & Shirts, P. 1997, ApJ, 474, L115

Butler, R. P., Marcy, G. W., Vogt, S. S., & Apps, K. 1998, PASP, 110, 1389

Cameron, A., Horne, K., Penny, A., & James, D. 1999, Nature, in press

Charbonneau, D., Noyes, R. W., Korzennik, S. G., Nisenson, P., Jha, S., Vogt, S. S., & Kibrick, R. I. 1999, ApJ, 522, L145

Fischer, D. A., Marcy, G. W., Bulter, R. P., Vogt, S. S., & Apps, K. 1999, PASP, 111, 50

Gilliland, R.L & Brown, T.M. 1992, PASP, 104, 582

Guillot, T., Burrows, A., Hubbard, W. B., Lunine, J. I., & Saumon, D. 1996, ApJ, 459, L35

Henry, G., Marcy, G., Butler, R. P., & Vogt, S. S. 1999, IAU Circ 7307

Mayor, M., Naef, D., Udry, S., Santos, N., Queloz, D., Melo, C., & Confino, B. 1999, http://obswww.unige.ch/~udry/planet/hd75289_ann.html

Mayor, M., & Queloz, D. 1995, Nature, 378, 355

Mazeh, T. et al. 2000, ApJ, in preparation (M00)

Queloz, D., et al. 1999, A&A, accepted, preprint available at http://xxx.lanl.gov/abs/astro-ph/9910223

Sackett, P. D. 1999, in NATO/ASI Ser., Planets Outside the Solar System: Theory and Observations, ed. J.-M. Mariotti & D. Alloin (Dordrecht: Kluwer), 189

Stetson, P. B. 1994, PASP, 106, 250

Udry, S., Mayor, M., Naef, D., Pepe, F., Queloz, D., Santos, N., & Burnet, M. 1999, http://obswww.unige.ch/~udry/planet/hd130322_ann.html

Vogt, S. S. et al. 1994, Proc. SPIE, 2198, 362

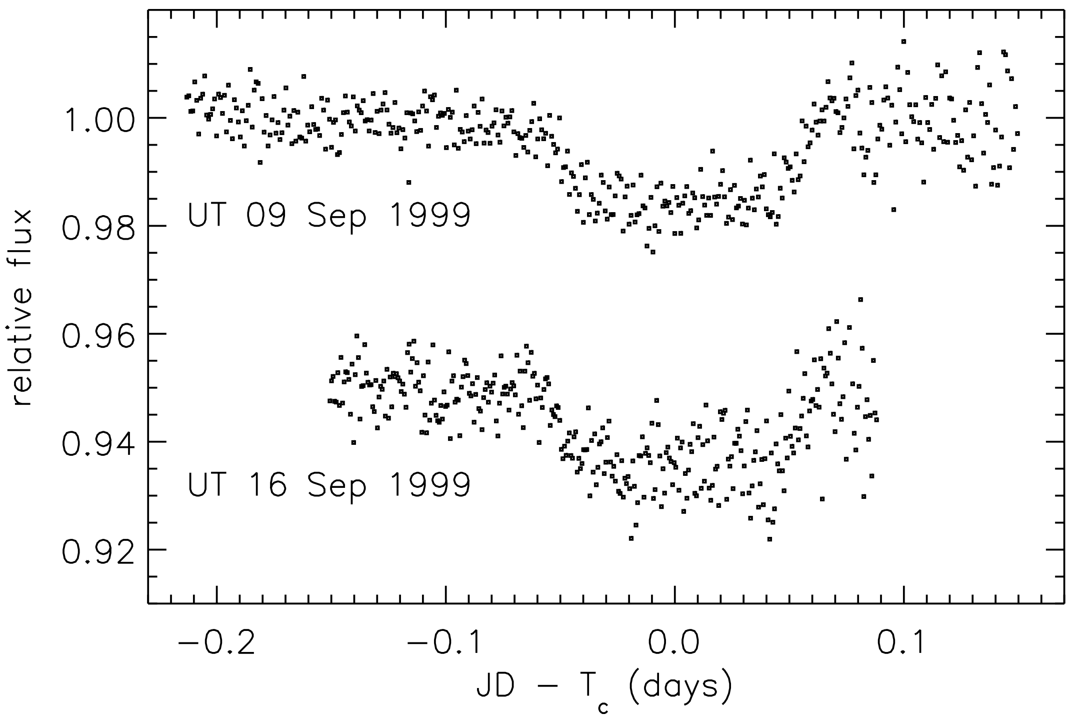

Fig. 1.— Shown are the photometric time series, corrected for gray and color-dependent extinction, for 9 & 16 Sep 1999, plotted as a function of time from T_c. The RMS of the time series at the beginning of the night on 9 Sep is roughly 4 mmag. The increased scatter in the 16 Sep data relative to the 9 Sep data is due to the shorter exposure times. The data from 16 Sep are offset by -.05 relative to those from 9 Sep.

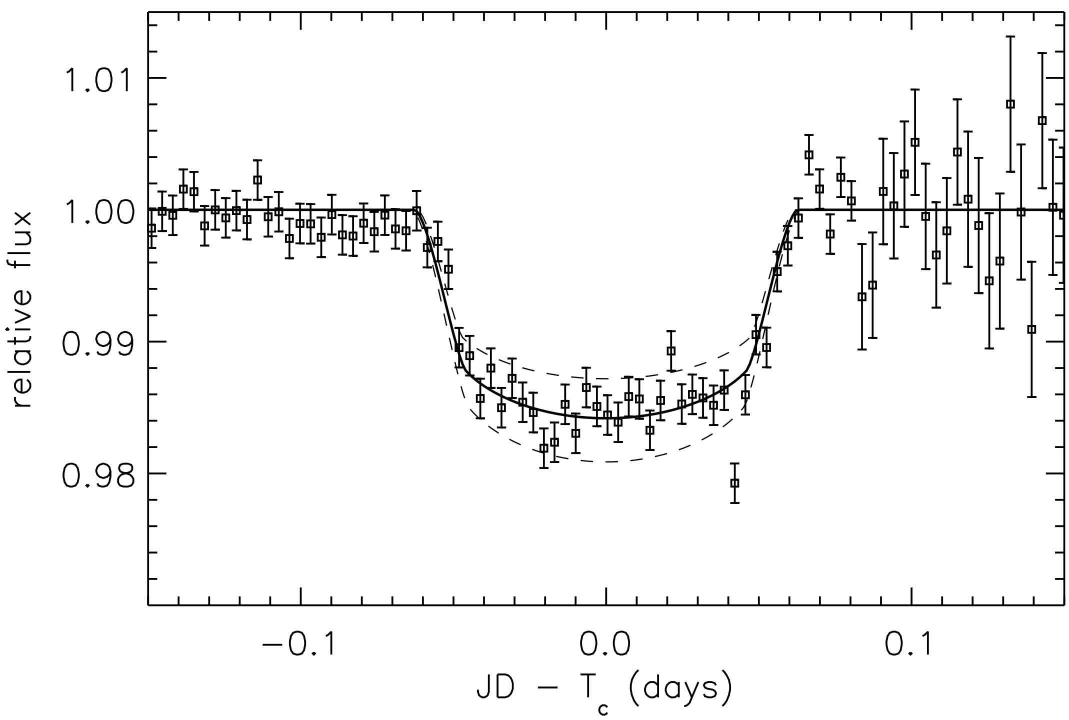

Fig. 2.— Shown are the data from figure 1 binned into 5 m averages, phased according to our best-fit orbit, plotted as a function of time from T_c. The RMS variation at the beginning of the time series is roughly 1.5 mmag, and this precision is maintained throughout the duration of the transit. The increased scatter at the end of the timeseries is due to increasing airmass which occured at roughly the same time for both transits, since the two occured very nearly one week apart. The solid line is the transit shape that would occur for our best fit model, $R_p = 1.27\ R_{\rm Jup}$, $i = 87.1°$. The lower and upper dashed lines are the transit curves that would occur for a planet 10% larger and smaller in radius, respectively. The rapid initial fall and final rise of the transit curve correspond to the times between first and second, and between third and fourth contacts, when the planet is crossing the edge of the star; the resulting slope is a function of the finite size of the planet, the impact parameter of the transit, and the limb darkening of the star. The central curved portion of the transit is the time between second and third contacts, when the planet is entirely in front of the star.

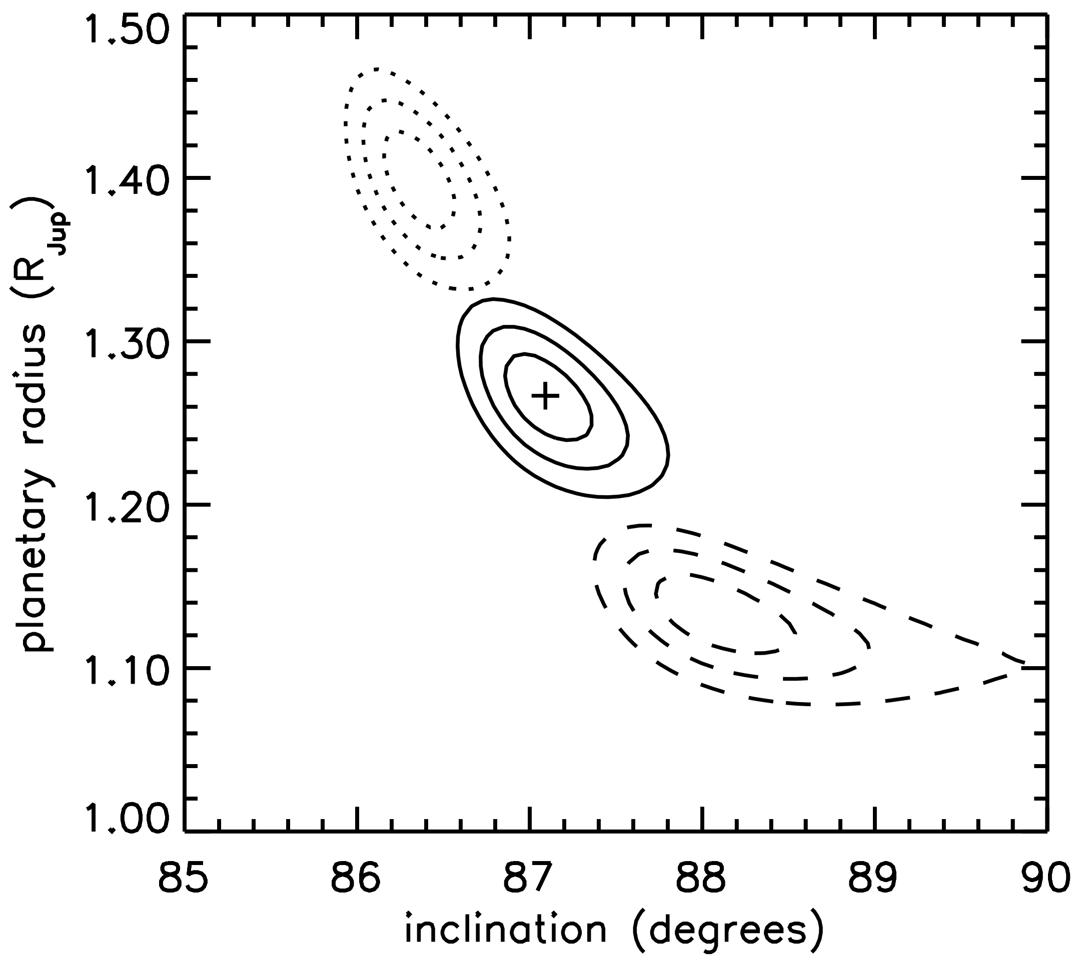

Fig. 3.— The solid contours are the 1-, 2-, & 3-σ confidence levels for the planet radius and orbital inclination, assuming $R_s = 1.1\ R_\odot$ and $M_s = 1.1\ M_\odot$. The minimum occurs at $R_p = 1.27\ R_{\rm Jup}$ and $i = 87.1°$. The dashed and dotted contours are the confidence levels in the cases of $\{R_s, M_s\} = \{1.0\ R_\odot, 1.0\ M_\odot\}$ and $\{R_s, M_s\} = \{1.2\ R_\odot, 1.2\ M_\odot\}$ respectively. The dominant modeling uncertainty is that in the stellar radius.